

Quantifying subtle but persistent peri-spine inflammation in vivo to submicron cobalt–chromium alloy particles

Nadim James Hallab · Frank W. Chan ·
Megan L. Harper

Received: 17 June 2011 / Revised: 14 December 2011 / Accepted: 26 February 2012 / Published online: 10 March 2012
© Springer-Verlag 2012

Abstract

Purpose We evaluated the consequences of cobalt–chromium alloy (CoCr) wear debris challenge in the peri-spine region to determine the inflammation and toxicity associated with submicron particulates of CoCr-alloy and nickel on the peri-spine.

Methods The lumbar epidural spaces of ($n = 50$) New Zealand white rabbits were challenged with: 2.5 mg CoCr, 5.0 mg CoCr, 10.0 mg CoCr, a positive control (20.0 mg of nickel) and a negative control (ISOVUE-M-300). The CoCr-alloy and Ni particles had a mean diameter of 0.2 and 0.6 μm , respectively. Five rabbits per dose group were studied at 12 and 24 weeks. Local and distant tissues were analyzed histologically and quantitatively analyzed immunohistochemically (TNF- α and IL-6).

Results Histologically, wear particles were observed in all animals. There was no evidence of toxicity or local irritation noted during macroscopic observations in any CoCr-dosed animals. However, Ni-treated control animals experienced bilateral hind leg paralysis and were euthanized at Day 2. Histopathology of the Ni particle-treated group revealed severe neuropathy. Quantitative immunohistochemistry demonstrated a CoCr-alloy dose-dependent

increase in cytokines (IL-6, TNF- α , $p < 0.05$) at 12 and 24 weeks.

Conclusions Subtle peri-spine inflammation associated with CoCr-alloy implant particles was dose dependent and persistent. Neuropathy can be induced by highly reactive Ni particles. This suggests peri-spine challenge with CoCr-alloy implant debris (e.g., TDA) is consistent with past reports using titanium alloy particles, i.e., mild persistent inflammation.

Keywords Spine · Osteolysis · Particles · Implant debris · Total disc arthroplasty · Cobalt–chromium alloy · Cytokines · Biological response

Introduction

The issue of metal debris released from prosthetic devices continues to be a source of concern, especially with the introduction of artificial discs and other motion preserving metal-on-metal devices in the spine [1, 21, 23]. It is generally recognized that implant-debris-induced aseptic loosening and periprosthetic osteolysis are the most common reasons for revision surgery [39]. Innate immune responses, i.e., macrophage responses, to implant debris mediate this osteolysis [9, 16, 20, 28, 33]. Past study of titanium particulates on the spine (dura) has demonstrated increased cytokines (e.g., TNF- α), increased osteoclastic activity and cellular apoptosis [7]. To date, similar in vivo investigation has not been reported with CoCr-alloy particles, despite the widespread use of CoCr-alloy spine implants.

Metal-on-metal total disc arthroplasties and fusion implants have been shown to produce wear debris particles in both the micron and submicron sizes [13, 18, 27, 32, 35]. Recent retrieval analysis of metal-on-metal total disc

N. J. Hallab
Department of Orthopaedic Surgery, Rush University Medical
Center, 1735 West Harrison, Chicago, IL 60612, USA

N. J. Hallab (✉)
Department of Orthopedic Surgery, Rush Medical College,
1653 W. Congress Parkway, Chicago, IL 60612, USA
e-mail: nhallab@rush.edu

F. W. Chan · M. L. Harper
Restorative Therapies Group, Medtronic,
2600 Sofamor Danek Dr, Memphis, TN 38132, USA

arthroplasty debris by Guyer et al. [12] has reported the CoCr-alloy implant debris to be primarily in the submicron range. It remains unknown if bolus challenge with CoCr-alloy particulate will elicit a persistent inflammatory reaction in the peri-spine area; and if so, to what degree? We hypothesized that a bolus amount of CoCr-alloy metal wear debris will induce only short-term dose-dependent inflammation (i.e., no persistent histological evidence of gross osteolysis and neurological effects). We tested this hypothesis by quantitatively evaluating the local inflammatory responses of spinal implant CoCr-alloy particles and nickel (Ni) particles in an in vivo rabbit model with perioperative and postmortem radiographic, histologic, and quantitative immunocytochemical analyses. Nickel was chosen as a positive control because while known to be reactive [3, 19, 26, 31, 34, 37], it is also orthopedically relevant as minor component of CoCr-alloy and steel implant alloys.

Methods and materials

Animal model

Fifty male New Zealand white rabbits, 3.2–3.5 kg at selection, were used as test subjects. The animals were randomized into 5 different treatment groups and then further subdivided into two follow-up periods of 12 and 24 weeks (i.e., 5 animals per treatment per period). The treatment groups consisted of 2.5 mg CoCr-alloy (T1), 5.0 mg CoCr-alloy (T2), 10.0 mg CoCr-alloy (T3) per animal, a Ni-treated group (20.0 mg Ni per animal) and a negative control group (ISOVUE-M 300). Animal husbandry was conducted at NAMS (Northwood, OH); the protocol was approved by their Institutional Animal Care and Use Committee (IACUC).

A rabbit model was selected for three reasons: (1) current FDA and ISO requirements for new spine materials require rabbit testing on the dura, etc. (e.g., Guidance for Industry and FDA Staff-Class II Special Controls Guidance Document: Intervertebral Body Fusion Device Document issued on: June 12, 2007, <http://www.fda.gov/MedicalDevices/DeviceRegulationandGuidance>); (2) previous studies of spinal implant debris reactivity have used rabbit models, thus our results will be comparable to other biomaterials; and (3) a rabbit model has been previously validated as capable of demonstrating debris induced osteolysis and inflammation in the peri-spine [5, 7, 17, 29, 30, 36].

Particles

Submicron particles of CoCr-alloy (ASTM, F-75) and pure Ni were obtained (BioEngineering Solutions Inc, Oak Park,

IL) and characterized using low angle laser light scattering (LALLS, Microtrac-X100, Microtrac, Montgomeryville, PA) and scanning electron microscopy (SEM, 3000-SN, Hitachi, Pleasanton, CA) to qualitatively analyze particle size, shape and composition (energy dispersive analysis x-ray, Oxford Inca EDX system). The CoCr-alloy particles size ranged from 0.1 to 3.27 μm (average size 0.2 μm diameter) (Fig. 1), where approximately 99.7 % of the total number of particles were sub-micrometer in size ($<1 \mu\text{m}$). Ni particles ranged from 0.3 to 18.5 μm (average 0.6 μm diameter). SEM analysis for all particles showed the size was consistent with the LALLS analysis and the particles were granular and flake-like in shape. Sterile particles were shown to be free of endotoxin ($<0.01 \text{ UE}$), using Kinetic QCL assays (Pyrogen 5000 assay, Biowhittaker). Several past investigations have shown that for a given amount of mass, smaller particles (e.g., $<1 \mu\text{m}$) generally produce greater inflammation than larger particles (e.g., 10 μm), because there is over $10\times$ the total amount of particle (i.e., dose) [10, 24, 25]. Thus submicron particles were chosen to reflect higher more reactive doses of particles while maintaining clinical relevance in size.

Surgical procedure

All animals underwent physical and neurological examinations to confirm healthy normal status prior to the inclusion in the study. The rabbits were preanesthetized with an intramuscular injection of ketamine hydrochloride (34 mg/kg) and xylazine (5 mg/kg) and general anesthetic was administered to each animal at a dose of 0.6 ml/kg body weight. The rabbits were maintained under general anesthesia on isoflurane inhalation. Prophylactic antibiotic (Baytril 10 mg/kg) and analgesia (buprenorphine 0.02 mg/kg) was administered before and after surgery.

Using fluoroscopic guidance, a 20 gauge needle was placed into the epidural space of the lumbar region (L4/5). A syringe with approximately 50 μl of ISOVUE-M-300 radiopaque contrast solution (Bracco Diagnostics, Princeton, NJ) was injected to confirm correct needle position. The test article was suspended in ISOVUE-M 300, aspirated into a second syringe and injected into the epidural space. A third syringe containing ISOVUE-M 300 was attached and approximately 50 μl was injected to rinse the test suspension from the needle lumen.

Gross observations and histology

At the designated intervals (12 and 24 weeks), the rabbits were sedated with an intramuscular injection of acepromazine maleate (0.2 ml/kg). The rabbits were then euthanized and macroscopic observation of the viscera was conducted.

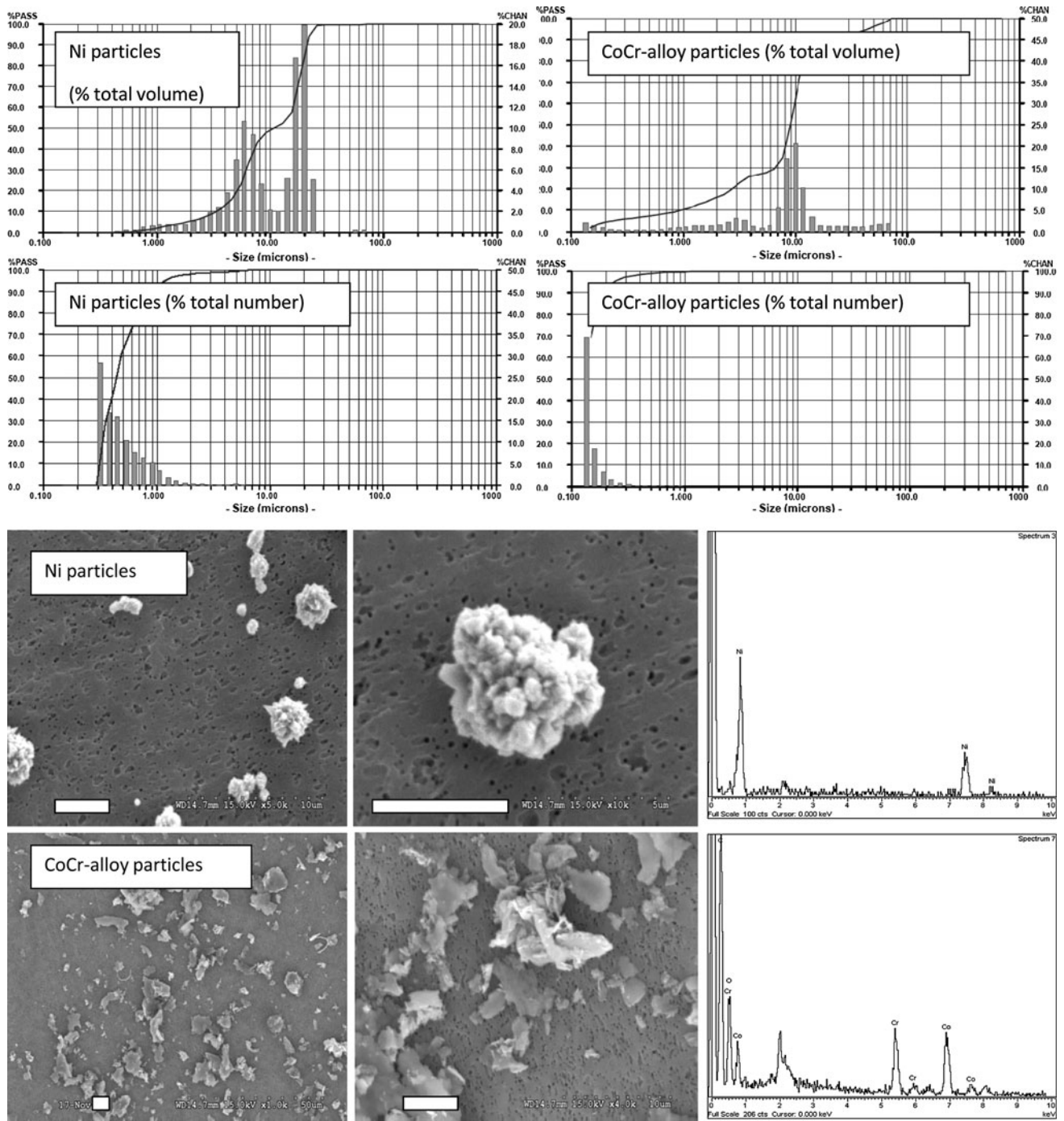


Fig. 1 Scanning electron micrographs (SEM), volume and number based LALLS size distributions and EDS determined chemical compositions for **a** CoCr-particles and **b** Ni particles, where CoCr-alloy particles had an average mean size = 0.2 µm diameter (number based), median = 0.14 µm, standard deviation of number distribution = 0.018 µm (overall range 0.1–74 µm). Ni particles had

an average mean = 0.6 µm diameter (number based), median = 0.42 µm, standard deviation of number distribution = 0.22 µm (overall range 0.3–74 µm). More than 99 % of the total number of CoCr-alloy particles were <1 µm and >94 % of Ni particles were <1 µm

The injected site along with several vertebrae levels cranial and caudal to the site and the muscle tissue immediately adjacent to the implant sites were dissected free and removed in toto. Additional tissues samples

including the brain, heart, lungs, liver, spleen, thymus, kidneys, adrenal glands, lymph nodes (mesenteric, sub-mandibular, and thoracic), gonads, and any tissue with visible gross lesions were gathered. All tissues were placed

in 10 % neutral buffered formalin paraffin-embedded, sectioned, stained with hematoxylin and eosin and evaluated by a qualified pathologist.

Immunohistochemistry

The guidelines for testing biological responses to particles (ASTM 1904-98, 2008) recommends measuring *in vivo* levels of cytokines using immunohistochemistry (IHC) of inflammatory cytokines such as IL-1 β , IL-2, IL-4, IL-6, IL-10, PGE₂, or TNF- α . Thus, a small section of the overlying tissue at the injection site was analyzed immunohistochemically for the expression of tumor necrosis factor-alpha (TNF- α) and interleukin-6 (IL-6). The frozen tissue was then fixed in 10 % formalin solution, paraffin-processed, and slide-mounted. These sections were treated with either anti-rabbit TNF- α or IL-6 (R&D Systems, and Santa Cruz Biochem) or left untreated.

Using primary and biotin linked secondary antibodies, immunohistochemical localization of IL-6 and TNF- α was performed. Briefly, treatment with cytokines involved dissolving the paraffin-embedded 10- μ m-thick tissue specimens using HistoSolv solution (Sigma, ST Louis, MO), followed by hydration with decreasing solutions of ethanol and water. Epitopes of IL-6 and TNF- α were retrieved with trypsin and blocked with 1.5 % goat (for TNF- α) or mouse (for IL-6) serum in PBS. The samples were incubated overnight with TNF- α or IL-6 primary antibodies at 4°C and stained using previously reported quantitatively IHC techniques [7, 17]. For each cytokine/time-point/control three slides per tissue specimen were analyzed from 5 randomly selected microscope fields per slide resulting in 15 fields per tissue sample (at 200 \times) that were used to quantify local cytokines (Scion Image, Scion Corporation, Frederick, MD). The total area of stained pixels was compared to the total pixel area of the microscope images. Standard two-tailed *t* testing was used to determine *p* confidence values of significance in cytokine expression between independent rabbit groups at each time point (12 and 24 weeks).

Results

Clinical observations

Postoperatively all Ni-treated animals for both time intervals appeared listless and exhibited decreased responsiveness and by Day 2 all Ni-treated animals that had evidence of neurological deficit such as bilateral hind leg paralysis and were euthanized. Otherwise all other animals appeared normal and there was no evidence of neurological deficit or other neurologic or musculoskeletal abnormalities following the surgical procedure.

Histology

Wear debris was present at the injection site of all Ni-treated and almost all test animals (Fig. 2). In addition, wear debris

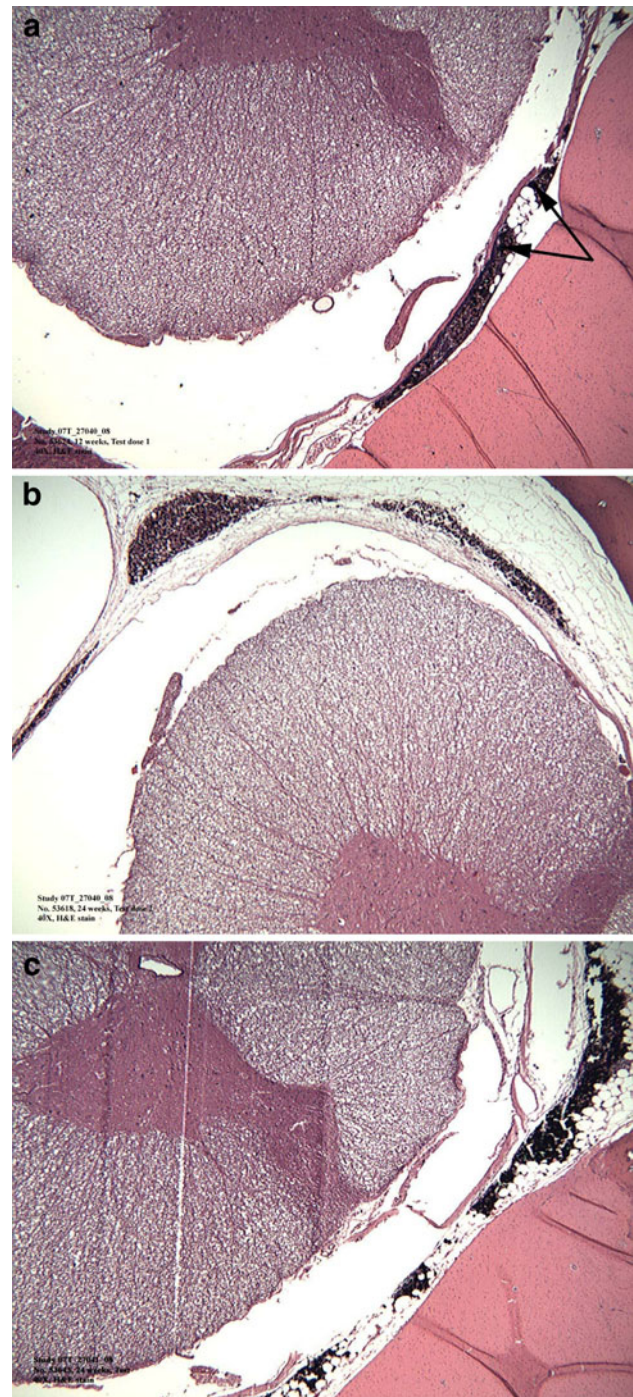


Fig. 2 Spinal cord sections from the implantation site showing CoCr-particles present in the areas around the implants, shown as black granular areas indicated by arrows: **a** 2.5 mg dose at 24 weeks, **b** 5.0 mg dose at 12 weeks, and **c** 10.0 mg dose at 24 weeks. Most of the wear debris challenge remained within the epidural region and was not extensively systemically distributed

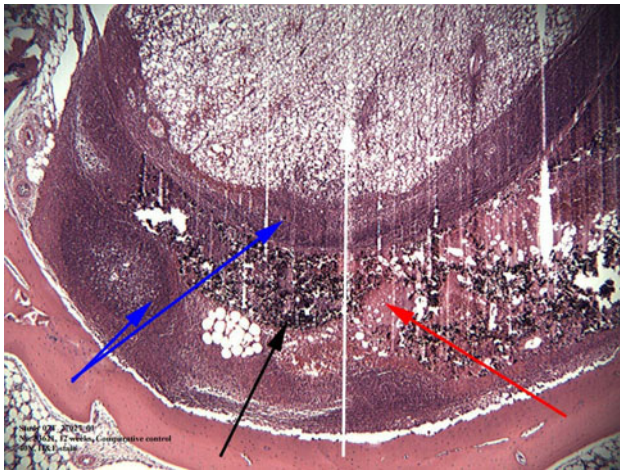


Fig. 3 Injection site of a Ni-treated animal at Day 2 with marked infiltration of polymorphonuclear cells (blue arrow) and moderate hemorrhage (red arrow) are observed around Ni particles (black arrow) and mild degeneration/necrosis (white arrow) observed in the spinal cord

was present in tissue samples from the segments located cranial and/or caudal to the injection site for all Ni-treated animals and most CoCr-alloy test animals regardless of dose.

Most of the wear debris was located within the epidural region in the cytoplasm and those found in macrophages or multinucleated giant cells (histiocytic inflammatory cells) for all CoCr-alloy-treated animals regardless of dose (Fig. 3). Minimal or mild epidural fibrosis consistent with a minimal fibrotic response to both the injection procedure and the wear debris was noted in T3 animals at 12 (5/5) and 24 (4/5) weeks. There were no adverse tissue effects such as necrosis, degeneration, infection/abscess formation, excessive inflammation, or unusual immune reaction in response to the wear debris particles in all but one T3 animal (animal euthanized on Day 8).

No systemic CoCr-alloy-related tissue alterations or particles were observed in distant organs associated (brain, heart, lungs, liver, adrenal glands, spleen, thymus, kidneys, thoracic lymph nodes, submandibular lymph nodes, mesenteric lymph nodes, and gonads).

Adverse tissue effects to the Ni debris included degeneration, and necrosis and hemorrhage were observed in the spinal cord, nerve roots and perivertebral region (Fig. 3). In one Ni-treated animal, there was a marked amount of polymorphonuclear cells surrounding the debris. Minimal to mild mixed cell infiltration was seen in the heart of all Ni-treated animals. This infiltration was thought to be secondary to severe inflammatory reaction observed at the injection site as no wear debris was seen in the heart.

Immunohistochemistry

The cytokines (antigens) localized on macrophages produced a brown chromogen label in response to primary and

secondary antibody treatment of TNF- α and IL-6. The regions of active cytokines were quantified using threshold image analysis of transmission light micrographs, showing detectable evidence of local IL-6 and TNF- α staining with the graphical analysis of percent area staining (Fig. 4).

Generally, there were statistically increased amounts of TNF- α and IL-6 observed in the rabbit tissue specimens from Ni-challenged and CoCr-alloy-challenged groups when compared to control animals, where 2-day Ni-challenged tissues demonstrated the greatest amounts of TNF- α and IL-6 staining on a non-normalized basis (Fig. 5). At 12 weeks all three CoCr-alloy-treated groups demonstrated increased amounts of TNF- α and IL-6 levels when compared to control tissues ($p < 0.05$). This increased expression of IL-6 and TNF- α is also visually identifiable in the processed images of the micrographs (Fig. 4). There were no significant dose-dependent responses between the elevated cytokine expressions of CoCr-alloy groups challenged with 2.5, 5.0, or 10.0 mg per rabbit at 12 or 24 weeks. The overall expression of IL-6 and TNF- α in particle-treated tissues was not statistically different between the 12- and 24-week samples on a non-normalized basis (Fig. 5). Secondary antibody controls were also used alone as controls, to account for any non-specific secondary antibody staining, $<0.01\%$.

Treated groups were normalized to nontreated controls at 12 and 24 weeks by dividing each cytokine value by the average of percent stain for non-treated controls (Fig. 6) where results of the non-treated controls are reduced to a cytokine index of 1. The resulting comparison demonstrates a statistical increase ($p < 0.03$) in the amount of IL-6 and TNF- α staining at 24 weeks, compared to 12 weeks. This increased response at 24 weeks over that at 12 weeks was only apparent at the higher doses (5 mg/rabbit and 10 mg/rabbit) for TNF- α . The cytokine index for the 5.0 and 10.0 mg CoCr-alloy groups were approximately threefold greater at 24 weeks than at 12 weeks, indicating a persistence or relative-increase in inflammation associated with particle challenge.

Discussion

The results did not support our original hypothesis, but indicated that while CoCr-alloy metal debris did not demonstrate osteolysis, it did produce a persistent subtle immune response. There was no histological evidence of gross toxicity or excessive local irritation noted in any of the CoCr-alloy dosed animals at 12- and 24-week time intervals. This is the first study of CoCr-alloy-induced effects in the peri-spine region [6]. However, our results are consistent with past investigation of peri-spine implant debris such as magnesium particles [22], titanium particles

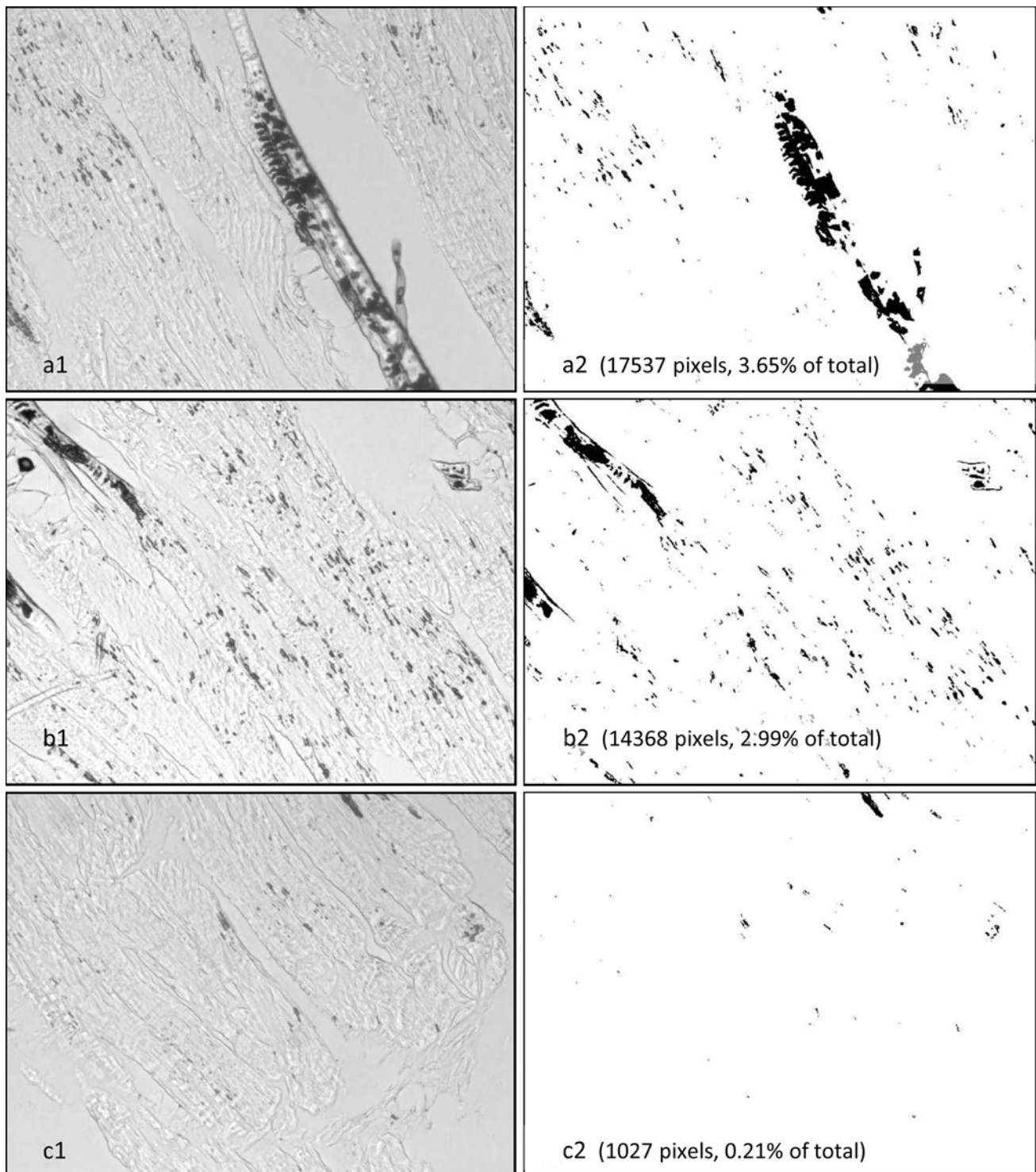


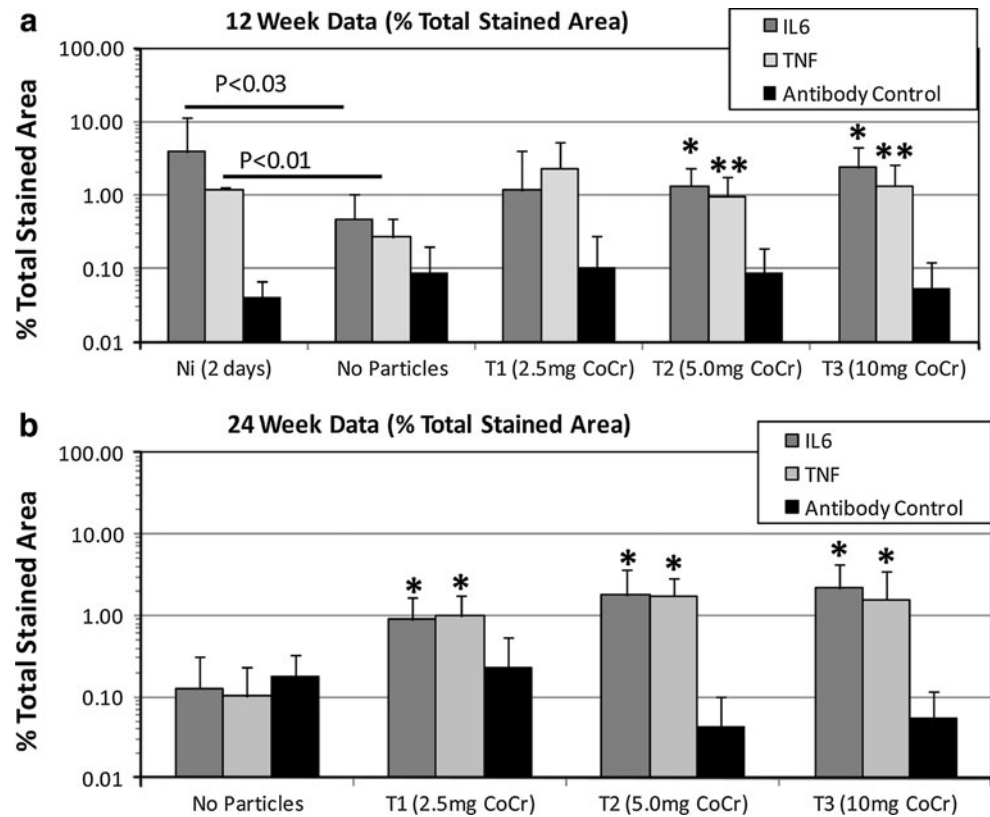
Fig. 4 Example of original microscope images (*left*) and image processed thresholded images (*right*) of areas of TNF- α staining used to calculate aerial percentages (*left*) and resulting images used for pixel quantification (*right*) for sample 53625-6-TNF (12 weeks,

10.0 mg CrCo dose). These images represent 3 of 15 images used to characterize TNF- α expression for a single tissue specimen, where 5 images for each of 3 tissue sections (slides) were used to characterize TNF- α expression in a single tissue

[7] and PEEK particles [30, 36]. These past in vivo investigations of spinal implant particles demonstrated that clinically relevant particles elicit chronic mild inflammatory

reactions [5, 7, 17, 29, 30]. Similar to our results, TNF- α was previously identified as a locally elevated cytokine associated with debris and peri-posterolateral arthrodesis [7, 38].

Fig. 5 12- and 24-week data showing percent of total stained area for each cytokine treatment with IL-6 or TNF- α (or control) for each Ni and CoCr dose. Statistically increased ($p < 0.05$) amounts of TNF- α and IL-6 were produced in Ni-challenged and CoCr-alloy challenged groups when compared to control animals, where 2-day Ni-challenged tissues demonstrated the greatest amounts of TNF- α and IL-6 staining on a non-normalized basis. * $p < 0.01$ when compared to non-treated control samples (no particles group) and ** $p < 0.03$ when compared to non-treated control samples (no particles group)

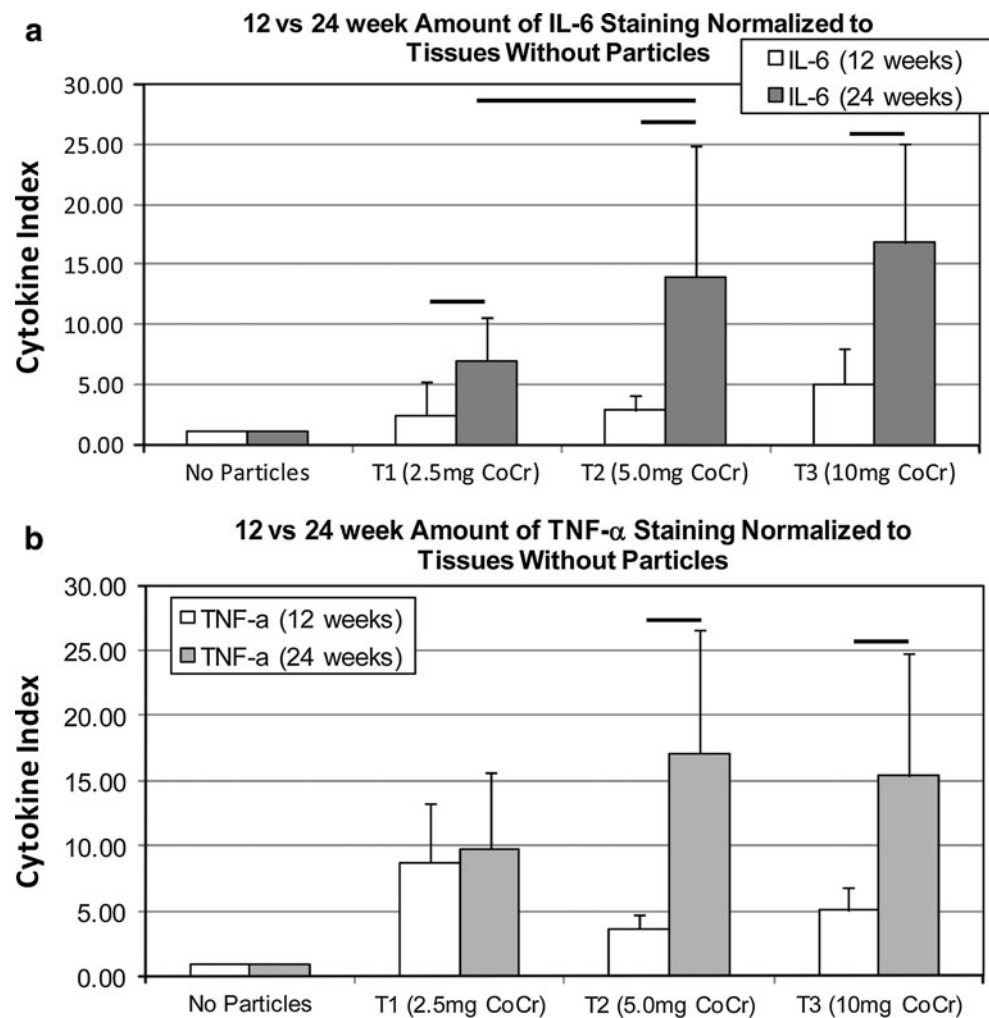


Continued particle-induced inflammation over the long term leads to inflammation, induced osteolysis and implant loosening [11].

This is the first report of reactive metal particles (Ni) used as a positive control in an animal model of implant debris inflammation (that are also a constituent of CoCr and stainless steel orthopedic alloys). This attempt to establish a baseline for what is an unacceptable level of particle-induced inflammation was only partially successful. This is because unexpected severe neuropathy developed in Ni-challenged rabbits (20 mg/rabbit Ni). This novel response thus demonstrated that of certain kinds of metal particles can have neuropathologic consequences in the peri-spine region. In contrast, there was little reactivity to CoCr-alloy debris at much longer exposure durations (Figs. 2, 3). This severe reaction to Ni was unexpected because past investigation by Rhalmi et al. [29] had previously shown that Nitinol particles (comprised of Ti with as high as 35 % Ni), were similarly non-reactive in peri-spine tissue when compared to pure Ti particles without Ni. The histopathology of Ni-treated animals (Fig. 3) revealed evidence of a toxic and/or inflammatory response with adverse tissue effects such as degeneration, necrosis, and hemorrhage in the spinal cord, nerve roots and perivertebral regions. As early as Day 2 there were significantly elevated amounts of IL-6 and TNF- α cytokines in the

Ni-treated local tissues when analyzed using quantitative immunohistochemistry. The Ni-treated animals had bilateral hind leg paralysis and had to be euthanized at Day 2, indicating that a bolus of 20 mg Ni was highly toxic and too high a dose to act as an effective “positive” control and model unacceptable long-term biologic effects. Nickel has been shown to be both immunogenic and carcinogenic in humans [4, 14]. In animal studies Ni has been shown to compete with Ca(2+) and induce mortality through whole body reductions in Na(+) [2]. However, the observance of Ni-induced neuropathy in the current investigation is a novel finding that needs to be further elucidated. While Ni is present in CoCr-alloy implants in <1 % (ASTM F75) and 10–15 % in stainless steel orthopedic implants (ASTM 316LV), the role of nickel in implant failure has not been investigated, aside from hypersensitivity responses [15]. Our attempt to define a level of “too much” inflammation (using Ni) is important for comparative purposes, but the dose we used (20 mg/rabbit) was too high, due to the unexpectedly high reactivity of Ni particles. Why Ni is so much more bioreactive/toxic than CoCr is largely unknown. Future experiments using Ni particle as a positive control in osteolysis studies should use a lower dosage (<10 mg) to facilitate longer observation out to 24-week time points. This will require extra caution and vigilant animal husbandry to prevent rabbit suffering.

Fig. 6 Co-Cr treated groups were normalized to nontreated controls at 12 and 24 weeks for (a) IL-6 and (b) TNF- α by dividing each sample cytokine value by the average percent stain for all non-treated samples at that time point. Non-treated controls are reduced to a cytokine index of 1. Lines indicate statistical difference between groups at $p < 0.03$. Dose-dependent differences were observed between 2.5 and 5 mg for IL-6 and between 2.5 and 10 mg for TNF- α



Negative control/sham surgeries using saline and X-ray contrast medium produce some measure of initial inflammation that was measurable at 12 weeks but not at 24 weeks. Particle-treatment groups that were normalized to this control data demonstrated strong dose dependence of cytokine increases associated with an increase in particle dose at 24 weeks ($p < 0.03$) but not at 12 weeks. This persistence of CoCr-alloy-induced inflammatory responses is subtle requiring both quantitative immunohistochemistry and normalization to non-treated controls to detect induced inflammatory reactions.

Clinically, our findings suggest that the various metals within implant alloys can have radically different reactivity profiles in vivo, particularly in the spine. There have been case reports of rare neurologic symptoms secondary to metallosis and granulomas produced by metallic spine implant debris [35]. For the first time, the risk of severe neuropathy by highly reactive metal particles has now been reproduced in vivo in an animal model, albeit by Ni particles not CoCr-alloy. Thus, while rare, our results demonstrate the ability of implant debris to produce neurologic

symptoms, increasing the grounds for enhanced surveillance when peri-spine metallosis is suspected.

Conclusions

The effects of spinal implant debris from wear and corrosion on local and systemic tissues remains a clinical concern. Reportedly, spinal implant debris elicits a macrophage-mediated response with increased levels of local pro-inflammatory cytokines, osteoclastogenesis and cellular apoptosis [8, 13, 29, 40]. The results of this in vivo study support this and this response is both dose dependent and can persist over the long term. These inflammatory responses to CoCr-particles were characterized by mild macrophage, lymphocyte and multinuclear cell infiltration in contrast to the observed neuropathologic responses to Ni particles. This is the first report of peri-spine tissue reactivity to CoCr-alloy particles in a rabbit animal model. Quantitative immunohistochemistry was able to discern particle-induced inflammation, at levels where traditional

histological examination of immune reactivity and serum cytokine analysis were unable to detect dose-dependent differences [7]. This study provides a basis for comparison of other implant materials in the spine and unexpectedly demonstrated the severe neuropathology that can be induced by submicron nickel particles. Further in vivo study is required to understand how much in vivo persistent inflammation is too much and when does it translate into osteolysis and spinal implant loosening.

Conflict of interest Conflicts of interest include that the N.J. Hallab is a paid consultant for Medtronic and F.W. Chan and M.L. Harper are employees of Medtronic which sells metal implants.

References

1. Agins H, Alcock NW, Bansal M, Salvati EA, Wilson PD, Pellicci PM, Bullough PG (1988) Metallic wear in failed titanium-alloy total hip replacements. A histological and quantitative analysis. *J Bone Joint Surg Am* 70-A:347–356
2. Alsop D, Wood CM (2011) Metal uptake and acute toxicity in zebrafish: common mechanisms across multiple metals. *Aquat Toxicol* 105:385–393
3. Caicedo M, Jacobs JJ, Reddy A, Hallab NJ (2007) Analysis of metal ion-induced DNA damage, apoptosis, and necrosis in human (Jurkat) T-cells demonstrates Ni(2+) and V(3+) are more toxic than other metals: Al(3+), Be(2+), Co(2+), Cr(3+), Cu(2+), Fe(3+), Mo(5+), Nb(5+), Zr(2+). *J Biomed Mater Res A* 86:905–913
4. Cameron KS, Buchner V, Tchounwou PB (2011) Exploring the molecular mechanisms of nickel-induced genotoxicity and carcinogenicity: a literature review. *Rev Environ Health* 26:81–92
5. Chang BS, Brown PR, Sieber A, Valdevit A, Tateno K, Kostuik JP (2004) Evaluation of the biological response of wear debris. *Spine J* 4:239S–244S
6. Cunningham BW (2004) Basic scientific considerations in total disc arthroplasty. *Spine J* 4:219S–230S
7. Cunningham BW, Orbegoso CM, Dmitriev AE, Hallab NJ, Seftor JC, McAfee PC (2002) The effect of titanium particulate on development and maintenance of a posterolateral spinal arthrodesis: an in vivo rabbit model. *Spine* 27:1971–1981
8. Denaro V, Papapietro N, Sgambato A, Barnaba SA, Ruzzini L, Paola BD, Rettino A, Cittadini A (2008) Periprosthetic electrochemical corrosion of titanium and titanium-based alloys as a cause of spinal fusion failure. *Spine* 33:8–13
9. Goodman SB (2007) Wear particles, periprosthetic osteolysis and the immune system. *Biomaterials* 28:5044–5048
10. Green TR, Fisher J, Matthews JB, Stone MH, Ingham E (2000) Effect of size and dose on bone resorption activity of macrophages by in vitro clinically relevant ultra high molecular weight polyethylene particles. *J Biomed Mater Res* 53:490–497
11. Gristina AG (1994) Implant failure and the immuno-incompetent fibro-inflammatory zone. *Clin Orthop* 298:106–118
12. Guyer RD, Shellock J, MacLennan B, Hanscom D, Knight RQ, McCombe P, Jacobs JJ, Urban RM, Bradford D, Ohnmeiss DD (2011) Early failure of metal-on-metal artificial disc prostheses associated with lymphocytic reaction: diagnosis and treatment experience in four cases. *Spine (Phila Pa 1976)* 36:E492–E497
13. Hallab NJ (2009) A review of the biologic effects of spine implant debris: fact from fiction. *SAS J* 3:143–160
14. Hallab N (2001) Metal sensitivity in patients with orthopedic implants. *J Clin Rheumatol* 7:215–218
15. Hallab N, Merritt K, Jacobs JJ (2001) Metal sensitivity in patients with orthopaedic implants. *J Bone Joint Surg Am* 83-A:428–436
16. Hallab NJ, Anderson S, Stafford T, Glant T, Jacobs JJ (2005) Lymphocyte responses in patients with total hip arthroplasty. *J Orthop Res* 23:384–391
17. Hallab NJ, Cunningham BW, Jacobs JJ (2003) Spinal implant debris-induced osteolysis. *Spine* 28:S125–S138
18. Hallab NJ, Khandha A, Malcolmson G, Timm JP (2008) In vitro assessment of serum–saline ratios for fluid simulator testing of highly modular spinal implants with articulating surfaces. *SAS Journal* 2:171–183
19. Hayes RB (1997) The carcinogenicity of metals in humans. *Cancer Causes Control* 8:371–385
20. Jacobs JJ, Hallab NJ (2006) Loosening and osteolysis associated with metal-on-metal bearings: a local effect of metal hypersensitivity? *J Bone Joint Surg Am* 88:1171–1172
21. Jacobs JJ, Urban RM, Schajowicz F, Gavrilovic J, Galante JO (1992) Particulate-associated endosteal osteolysis in titanium-base alloy cementless total hip replacement. Particulate debris from medical implants. *Am Soc Test Mater* 1992:52–60
22. Kaya RA, Cavusoglu H, Tanik C, Kaya AA, Duygulu O, Mutlu Z, Zengin E, Aydin Y (2007) The effects of magnesium particles in posterolateral spinal fusion: an experimental in vivo study in a sheep model. *J Neurosurg Spine* 6:141–149
23. Lombardi AV Jr, Mallory TH, Vaughn BK, Drouillard P (1989) Aseptic loosening in total hip arthroplasty secondary to osteolysis induced by wear debris from titanium-alloy modular femoral heads. *J Bone Joint Surg* 71-A:1337–1342
24. Matthews JB, Besong AA, Green TR, Stone MH, Wroblewski BM, Fisher J, Ingham E (2000) Evaluation of the response of primary human peripheral blood mononuclear phagocytes to challenge with in vitro generated clinically relevant UHMWPE particles of known size and dose. *J Biomed Mater Res* 52:296–307
25. Matthews JB, Green TR, Stone MH, Wroblewski BM, Fisher J, Ingham E (2000) Comparison of the response of primary murine peritoneal macrophages and the U937 human histiocytic cell line to challenge with in vitro generated clinically relevant UHMWPE particles. *Biomed Mater Eng* 10:229–240
26. Nonaka H, Nakada T, Iijima M, Maibach HI (2011) Metal patch test results from 1990–2009. *J Dermatol* 38:267–271
27. Pare PE, Chan F, Powell ML (2007) Wear characterization of the A-MAVTM anterior motion replacement using a spine wear simulator. *Wear* 263:1055–1059
28. Ren W, Wu B, Peng X, Hua J, Hao HN, Wooley PH (2006) Implant wear induces inflammation, but not osteoclastic bone resorption, in RANK(-/-) mice. *J Orthop Res* 24:1575–1586
29. Rhalmi S, Charette S, Assad M, Coillard C, Rivard CH (2007) The spinal cord dura mater reaction to nitinol and titanium alloy particles: a 1-year study in rabbits. *Eur Spine J* 16:1063–1072
30. Rivard CH, Rhalmi S, Coillard C (2002) In vivo biocompatibility testing of peek polymer for a spinal implant system: a study in rabbits. *J Biomed Mater Res* 62:488–498
31. Samitz MH, Klein A (1973) Nickel dermatitis hazards from prostheses. *J Am Med Assoc* 223:1159
32. Senaran H, Atilla P, Kaymaz F, Acaroglu E, Surat A (2004) Ultrastructural analysis of metallic debris and tissue reaction around spinal implants in patients with late operative site pain. *Spine (Phila Pa 1976)* 29:1618–1623
33. Shanbhag AS, Kaufman AM, Hayata K, Rubash HE (2007) Assessing osteolysis with use of high-throughput protein chips. *J Bone Joint Surg Am* 89:1081–1089
34. Summer B, Paul C, Mazoochian F, Rau C, Thomsen M, Banke I, Gollwitzer H, Dietrich KA, Mayer-Wagner S, Ruzicka T, Thomas P (2010) Nickel (Ni) allergic patients with complications to Ni containing joint replacement show preferential IL-17 type reactivity to Ni. *Contact Dermatitis* 63:15–22

35. Takahashi S, Delecrin J, Passuti N (2001) Intraspinal metallosis causing delayed neurologic symptoms after spinal instrumentation surgery. *Spine (Phila Pa 1976)* 26:1495–1498
36. Utzschneider S, Becker F, Grupp TM, Sievers B, Paulus A, Gottschalk O, Jansson V (2010) Inflammatory response against different carbon fiber-reinforced PEEK wear particles compared with UHMWPE in vivo. *Acta Biomater* 6:4296–4304
37. Vollmer J, Weltzien HU, Gamerding K, Lang S, Choleva Y, Moulon C (2000) Antigen contacts by Ni-reactive TCR: typical alpha chain cooperation versus alpha chain-dominated specificity. *Int Immunol* 12:1723–1731
38. Wang JC, Yu WD, Sandhu HS, Betts F, Bhuta S, Delamarter RB (1999) Metal debris from titanium spinal implants. *Spine* 24:899–903
39. Willert HG, Semlitsch M (1977) Reactions of the articular capsule to wear products of artificial joint prostheses. *J Biomed Mater Res* 11:157–164
40. Xu R, Ebraheim NA, Nadaud MC, Phillips ER (1996) Local tissue of the lumbar spine response to titanium plate–screw system. Case reports. *Spine* 21:871–873